

Cite this: DOI: 10.1039/c0xx00000x

www.rsc.org/xxxxxx

ARTICLE TYPE

Broadband cavity-enhanced absorption spectroscopy for real time, *in situ* spectral analysis of microfluidic droplets

Simon R.T. Neil,^a Cathy M. Rushworth,^b Claire Vallance,^{b*} and Stuart R. Mackenzie^{a*}

Received (in XXX, XXX) Xth XXXXXXXXXX 20XX, Accepted Xth XXXXXXXXXX 20XX

DOI: 10.1039/b000000x

Broadband cavity enhanced absorption spectroscopy has been used to record, in real time, the absorption spectrum of microliter volume aqueous phase droplets within a microfluidic chip assembly. Using supercontinuum radiation and broadband coated external mirrors, the full visible spectrum ($430 < \lambda/\text{nm} < 700$) of each passing droplet is acquired *in situ* at high repetition rates (273 Hz / 3.66 ms acquisition time) and high sensitivity ($\alpha_{\text{min}} < 10^{-2} \text{ cm}^{-1}$). The possibilities for further improvements in sensitivity and acquisition rate using custom designed chips are discussed.

A wide variety of optical detection methods have been applied to microfluidic systems, including fluorescence, absorbance, chemiluminescence, surface plasmon resonance, and Raman spectroscopy.¹ In the analysis of macroscopic chemical samples, direct absorbance spectroscopy is considered a universally applicable analytical technique. Its application to microfluidic systems, however, presents significant challenges due to the dramatically reduced optical pathlengths involved. Liquid-core waveguides and fiber optics have been employed to guide light through microchannels in order to increase the optical pathlength sampled.^{2, 3} However, whilst waveguide-based approaches are well suited to integration within microfluidic devices, paving the way for commercially viable “on-chip” techniques in which the light source, fluidic elements and detector are all incorporated within a single monolithic platform,^{1, 4, 5} they remain relatively insensitive compared with other on-chip optical detection methods. Furthermore, the integration of waveguides places constraints on the chip and channel geometry and can introduce significant light losses during coupling and detection.

One convenient way to increase the effective path-length is to use multiple pass techniques. A simple way to achieve this is to place the sample within a high finesse optical cavity such as that formed between two highly reflective mirrors. Cavity-enhanced spectroscopic techniques of this type are well established in gas-phase absorbance measurements⁶ and are becoming increasingly popular for liquid phase studies.^{7, 8}

Integration of multiple-reflection mirrors into microfluidic chips has been achieved previously using coated capillaries⁹ or, for protein / bulk solution detection with integrated gold mirrors¹⁰ although difficulties in alignment led to modest gains in sensitivity compared with single pass measurements.

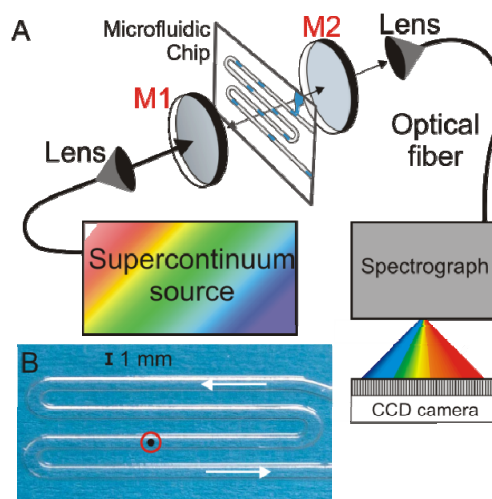


Fig. 1 (A) Experimental BBCEAS setup. (B) The microfluidic chip and channels (1 mm in width and 320 μm in depth), as viewed along the optical axis of the cavity. The position and estimated size of the optical beam is shown as a black dot.

Here we describe the first application of truly broadband cavity-enhanced absorption spectroscopy (BBCEAS) to *in situ* analyte detection within microfluidic droplets. In BBCEAS, broadband light is continually injected into an optical cavity formed between two broadband, highly reflective mirrors. The time-integrated light intensity emerging from the cavity, $I(\lambda)$, is dispersed into its constituent wavelengths before detection. For small intracavity light losses and high mirror reflectivities, the wavelength-dependent (decadic) absorbance $A = \epsilon Cl$, may be approximated from measurements made in the presence, I , and absence, I_0 , of a sample, as

$$2.3026 A = 2.3026 \epsilon Cl = \frac{(I_0/I) - 1}{\text{CEF}}, \quad (1)$$

where ϵ is the molar absorptivity, C the absorber concentration and l the single-pass optical pathlength through the sample.¹¹ CEF is the cavity-enhancement factor, defined as the ratio of the measured absorbance to that for a single pass.

The experimental setup used here is shown schematically in Fig. 1(A). Two highly reflective mirrors, M1 and M2, (Layertec, $R_{400-800 \text{ nm}} > 0.9985$, 1 m radius of curvature) form a stable linear cavity of length 12 cm. A microfluidic chip (Fig 1 B) is inserted into the optical cavity at normal incidence to the optical beam

such that the light within the cavity passes through a single microfluidic channel.

The microfluidic chip used in these experiments was fabricated according to Section 3 of Ref 12. Channels of width 1 mm and depth 320 μm were fabricated in UV-curing optical adhesive (Norland NOA81), sandwiched between two ~ 140 μm thick microscope cover slides. Liquid flows into and out of the chip through Nanoports (Upchurch Scientific). Dual inlets allow for measurements to be made in continuous- or droplet-flow regimes.

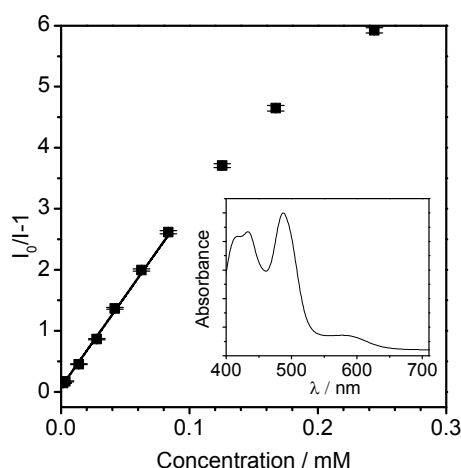


Fig. 2 $I_0/I - 1$ (at 487 nm) versus Ir(IV) concentration. Data points represent the average of 15 measurements, the standard deviation of which is shown. The solid line represents an error-weighted regression ($R^2 = 0.996$) through the linear region of the graph. Inset, normalized absorption spectrum of Ir(IV).

In order to record broadband spectra at high repetition rates a spectrally brilliant commercial supercontinuum (SC) source (NKT, Koheras SuperK Power Blue) is employed.^{13,14} Before entering the cavity, the light is spectrally filtered, yielding a bandwidth of 400 - 800 nm (300 mW visible output power). This matches the bandwidth of the high reflectivity mirror coatings. At its intersection with the chip, the beam diameter is *ca.* 600 μm , which, with the per-pass optical pathlength (l) through solution of 320 μm , yields a probed sample volume of ~ 90 nL.

Light exiting the cavity is fibre-coupled to a grating spectrograph (Andor Technology, SR-303i), which disperses its component wavelengths onto a CCD camera (Andor Technology, Newton). Spectra are acquired with a 3.66 ms acquisition time, at a repetition rate of 273 Hz. The data rate is limited only by the camera's acquisition settings / transfer rate. In other applications with more sophisticated cameras we have recorded full visible spectra with acquisition times of 10 μs at > 600 Hz.¹³

In this proof-of-principle demonstration, we monitored droplets or 'slugs' of aqueous K_2IrCl_6 solution (Ir(IV)), during their flow through a microfluidic channel in a toluene carrier phase. Before droplet-flow measurements, the detection sensitivity was determined in a series of single-wavelength continuous flow measurements. The absorption spectrum of Ir(IV), shown inset in Fig. 2, displays a maximum at 487 nm. The intensity, I , of 487 nm light transmitted through the cavity was recorded as solutions containing different concentrations of Ir(IV) were flowed continuously through the cell. The reference, I_0 , was determined from measurements with pure solvent flowing through the chip. Fig. 2 shows $I_0/I - 1$ as a function of $[\text{Ir(IV)}]$. At

low concentrations, the plot displays a linear dependence on concentration (*i.e.*, $I_0/I - 1 \propto A$), with curvature at higher concentrations which may be attributed to a breakdown in the approximations leading to Equation 1.^{14, 15} An error-weighted regression through the linear region provides a measure of the limit of detection (LOD) of 1.4 μM for Ir(IV), determined from the 3σ uncertainty on the intercept. The minimum detectable per-pass absorbance, A_{min} , is 1.8×10^{-4} . The absorption coefficient, α , is given by $\alpha = 2.3026\epsilon C$, where the C is the concentration and ϵ the extinction coefficient, equal to $4000 \text{ M}^{-1} \text{ cm}^{-1}$,¹⁶ for Ir(IV) at 487 nm. A limit of detection of $C_{\text{min}} = 1.4 \mu\text{M}$ corresponds to a minimum detectable absorption, α_{min} , of $1.3 \times 10^{-2} \text{ cm}^{-1}$.

To compare with single pass measurements, Equation (1) can be used to determine values for the CEF. At 487 nm the slope of the linear fit in Fig. 2 yields a CEF of 102, corresponding to an effective path length, $l_{\text{eff}} = \text{CEF} \times l$, of 3.26 cm. It is worth reiterating that this was achieved with a standard chip without any precision optical surfaces in just a 55 ms acquisition time. It is clear, even in these preliminary efforts, that the sensitivity of the BBCEAS technique surpasses that of previous absorption measurements in microfluidic chips (see, for example, Refs 1 and 17 and references therein).

In the present work, the number of light passes through the cavity is primarily limited by the poor optical quality of the microfluidic chip itself. In previous liquid-phase cavity-based studies, α_{min} values in the range $10^{-3} - 10^{-7} \text{ cm}^{-1}$ have been achieved using high quality optical components (see Table II in Ref 18), indicating that by improving the optical quality of the chip alone, there is scope to improve the measurement sensitivity by several orders of magnitude.

In addition to the small volumes probed and the high sensitivity, a major advantage of this approach is its spectral bandwidth. To illustrate these combined attributes, Fig. 3 shows the absorption spectrum of $\sim 6 \mu\text{L}$ 'slugs' of 40 μM aqueous Ir(IV) solution flowing rapidly (0.35 ml/min) through the chip in a toluene carrier phase. The temporal and wavelength-resolved spectra are shown in Fig. 3A. For these measurements, I_0 was the signal recorded in the presence of the carrier phase only. Fig. 3B highlights the excellent signal to noise achieved for an individual spectrum despite the short, 3.66 ms, acquisition time. The time resolution is demonstrated by the absorbance at 487 nm shown in Fig. 3C. Each individual spectrum contains a spectrally flat background component which we believe arises from scatter at the interface between the slug and a thin lubricating layer of carrier phase at the walls of the chip. As the absorption spectrum of Ir(IV) is known, this scattering contribution is easily quantified and subtracted (see Fig. 3B).

At both ends of the Ir(IV) slugs, lensing effects result in a large increase in the scattering. Only as the main body of the slug passes into the beam is the absorbance spectrum of Ir(IV) recovered, (Fig. 3B). The large scattering-induced signals at the start and end of each droplet provide convenient signals for triggering acquisition during droplet flow, and could potentially be exploited for droplet shape analysis.

The signal to noise ratio achieved permits an alternative estimate of α_{min} . From the 3σ uncertainty in the baseline of the plot in Fig 3C, $\alpha_{\text{min}}(487 \text{ nm})$ is estimated to be $9.5 \times 10^{-3} \text{ cm}^{-1}$, close to the value obtained from the fit to the data in Fig. 2.

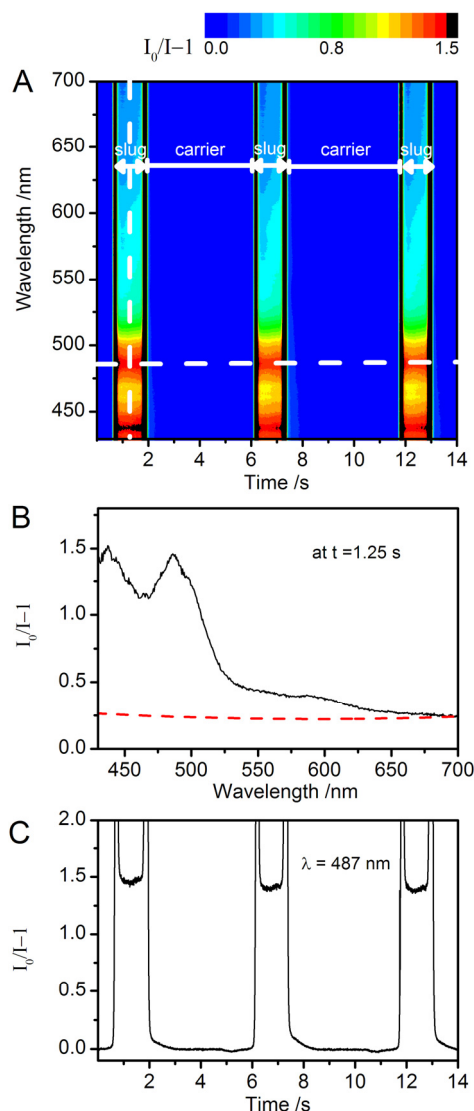


Fig. 3 (A) Contour plot of the BBCEAS-measured spectra as a function of time during a flow (0.35 mL min^{-1}) of Ir(IV) slugs through the microfluidic chip. (B) Spectral cut through the contour plot at 1.25 s (red dashed line represents a baseline scattering contribution) and (C) a temporal cut through at 487 nm.

Given the proof-of-principle nature of this study, it is pertinent to discuss the future potential, and the limitations, of BBCEAS for microfluidic sensing. One of the key factors not already discussed, which restricts the detection limit of the technique, is the stability of the supercontinuum source. Due to drift in the BBCEAS signal, increasing the signal integration time by a factor of 100, to 0.366 s, only results in a factor of two improvement in $\alpha_{\text{min}}(487\text{nm})$. The drift may be reduced by improving the chip and cavity design, but a significant component is inherent in the SC source itself. To some extent this is the price paid for the intense, broadband coverage. Rapid switching between I_0 and I may mitigate against this and would be well-suited to the study of rapidly flowing droplets.

As discussed above, the sensitivity of the technique is expected to improve markedly with minor modifications to the chip design (e.g., by incorporating optical quality surfaces). The large slug volumes used here could also be reduced substantially without

losing sensitivity by using chip designs and dimensions that more closely match the total droplet/slug volume with that probed by the cavity beam

A key advantage of the BBCEAS technique is that the broadband character of the absorption measurements allows the separation of contributions from species whose absorption spectra overlap. This may be potentially useful for probing reactions within droplets,¹⁹ and, coupled with the fast temporal response, we envisage the technique being of considerable value in studying intra-droplet kinetics.

In summary, these results represent the first application of broadband cavity-enhanced absorption spectroscopy to the analysis of microfluidic samples. The technique provides full visible broadband spectral measurement with both high detection sensitivity and excellent temporal and spatial resolution.

We would particularly like to thank Joanna Davies and Dr. João Cabral at Imperial College London for fabricating the chips used in this work. This work was funded by grants from EPSRC (EP/G027838/1), DARPA (QuBE: N66001-10-1-4061) and the EMF Biological Trust.

Notes and references

- ^a Department of Chemistry, University of Oxford, Physical and Theoretical Chemistry Laboratory, South Parks Road, Oxford OX1 3QZ, UK; e-mail stuart.mackenzie@chem.ox.ac.uk
- ^b Department of Chemistry, University of Oxford, Chemistry Research Laboratory, 12 Mansfield Rd, Oxford OX1 3TA, UK; e-mail claire.vallance@chem.ox.ac.uk
1. B. Kuswandi, Nuriman, J. Huskens and W. Verboom, *Anal. Chim. Acta*, 2007, **601**, 141-155.
2. K. B. Mogensen and J. P. Kutter, *Electrophoresis*, 2009, **30**, S92-S100.
3. P. J. Viskari and J. P. Landers, *Electrophoresis*, 2006, **27**, 1797-1810.
4. M. L. Adams, M. Enzelberger, S. Quake and A. Scherer, *Sens. Actuator A-Phys.*, 2003, **104**, 25-31.
5. L. Malic and A. G. Kirk, *Sens. Actuator A-Phys.*, 2007, **135**, 515-524.
6. G. Berden and R. Engeln (Eds), *Cavity Ring-Down Spectroscopy Techniques and Applications*, Wiley, 2009.
7. C. Vallance, *New J. Chem.*, 2005, **29**, 867-874.
8. M. Schnippering, S. R. T. Neil, S. R. Mackenzie and P. R. Unwin, *Chem. Soc. Rev.*, 2011, **40**, 207-220.
9. H. Salimi-Moosavi, Y. T. Jiang, L. Lester, G. McKinnon and D. J. Harrison, *Electrophoresis*, 2000, **21**, 1291-1299.
10. L. Billot, A. Plecis and Y. Chen, *Microelectron. Eng.*, 2008, **85**, 1269-1271.
11. G. Berden, R. Peeters and G. Meijer, *International Reviews in Physical Chemistry*, 2000, **19**, 565-607.
12. C. Harrison, J. T. Cabral, C. M. Stafford, A. Karim and E. J. Amis, *J. Micromech. Microeng.*, 2004, **14**, 153-158.
13. L. van der Sneppe, G. Hancock, C. Kaminski, T. Laurila, S. R. Mackenzie, S. R. T. Neil, R. Peverall, G. A. D. Ritchie, M. Schnippering and P. R. Unwin, *Analyst*, 2010, **135**, 133-139.
14. S. E. Fiedler, A. Hese and A. A. Ruth, *Rev. Sci. Instrum.*, 2005, **76**, 7.
15. S. E. Fiedler, A. Hese and A. A. Ruth, *Rev. Sci. Instrum.*, 2005, **76**, 1.
16. L. Moggi, G. Varani, M. F. Manfrin and V. Balzani, *Inorg. Chim. Acta*, 1970, **4**, 335-341.
17. C. F. A. Floquet, V. J. Sieben, A. Milani, E. P. Joly, I. R. G. Ogilvie, H. Morgan and M. C. Mowlem, *Talanta*, 2011, **84**, 235-239.
18. M. Islam, L. N. Seetohul and Z. Ali, *Appl. Spectrosc.*, 2007, **61**, 649-658.
19. L. N. Seetohul, Z. Ali and M. Islam, *Anal. Chem.*, 2009, **81**, 4106-4112.